Three-dimensional vibration patterns of alto saxophone reeds measured on different mouthpieces under mimicked realistic playing conditions

Reference:
Ukshini Enis, Dirckx Joris, Ukshini Enis.- Three-dimensional vibration patterns of alto saxophone reeds measured on different mouthpieces under mimicked realistic playing conditions
The journal of the Acoustical Society of America / Acoustical Society of America- ISSN 1520-8524 - Melville, 150:5(2021), p. 3730-3746
Full text (Publisher's DOI): https://doi.org/10.1121/10.0007281
To cite this reference: https://hdl.handle.net/10067/1839110151162165141

3D vibration patterns of alto saxophone reeds measured on different mouthpieces under mimicked realistic playing conditions

Enis Ukshini, Joris J.J. Dirckx,

Department of Physics, Laboratory of Biomedical Physics BIMEF, University of Antwerp, Groenenborgerlaan 171, Antwerp, 2020, Belgium

In single reed musical instruments, vibrations of the reed, in conjunction with the geometry of the mouthpiece and the acoustic feedback of the instrument, play an essential role in sound generation. Up till now, 3D reed vibration patterns have only been studied under external acoustic stimulation, or at a single note and lip force. This paper investigates vibration patterns of saxophone reeds under imitated realistic playing conditions. On different notes displacement measurements on the entire optically accessible part of the reed are performed using stroboscopic digital image correlation. These vibration data are decomposed onto the harmonic frequencies of the generated note pitch and into the operational modes. Motion data as a function of time are shown on single points. All points on the reed predominantly move in phase, corresponding to the first flexural mode of the reed. At higher note harmonics very low amplitude higher vibration modes are superimposed on the fundamental mode. Mouthpiece characteristics and lip force influence the vibration patterns. Vibration patterns differ strongly form earlier measurements on free vibrating reeds. Results show that single-point measurements on the tip of the reed can give a good indication of the 3D vibration amplitude, also at higher note pitches.

I. INTRODUCTION

Reeds used in woodwind instruments play a crucial role in the instrument's acoustic functioning as the reed's oscillation is the driving mechanism for the airflow modulation, and hence for the production of sound. In single-reed instruments such as the clarinet and the saxophone, the reed is a flat piece of natural or synthetic material, machined into a certain shape. The instrument mouthpiece has a long-shaped opening, which is largely closed by the reed lying on top of it. Towards its tip, the mouthpiece surface gradually bends down so that the distance between the reed and the mouthpiece sidewalls (also called "rails" or "facings) increases, leaving a slit-shaped opening at the tip of the mouthpiece. Drawings of mouthpieces explaining the terminology to indicate mouthpiece parts can be found in (Chen, 2009) and in Figure 2. The player's lower lip bends the reed towards the mouthpiece, and air is forced through the remaining opening. A complex interplay between reed mechanics, lip force, hydrodynamics of the airstream and acoustic properties of the mouthpiece and the instrument sets the reed into periodic motion. Under normal playing conditions, the instrument is the dominant oscillator and the reed locks in to the instruments acoustic frequency (Fletcher, 1978). Different combinations of opened and closed tone holes change the resonance characteristics of the instrument so that standing waves of different frequencies are excited.

The musical sound of the instrument depends strongly on the details of the reed's oscillation through one full periodic motion (Fabre et al., 2011). The reed in itself is a long-shaped slab and behaves as a multi-mode vibrating system (Campbell, 1999). Traditionally it is made out of natural cane, but in recent years synthetic materials have gained interest and use, as their mechanical properties are coming closer to the natural materials (Ukshini and Dirckx, 2020). Along its length the thickness of the reed is machined towards a very thin tip, and the cross-section changes from a bulge in the center to a uniform thickness at the tip. An important parameter is the stiffness of the reed towards its tip, which is indicated by a so-called "strength", but relationships between stiffness and strength number vary between manufacturers and reed shapes. The behavior of natural reeds can differ rather strongly between specimen and depends greatly on humidity, while with synthetic materials the mechanical properties of different specimens vary far less. The link between the objectively measured mechanical parameters of the reed and the subjective characterization of the sound has been studied in detail (Gazengel et al., 2016). In the study correlation coefficients between subjective descriptors and mechanical parameters were retrieved. A strong correlation was shown between the mechanical parameters and the perceived quality of the reeds. Actual stiffness of individual cane reeds can differ rather strongly from one sample to the next. The material parameters of high-quality synthetic reeds are far more constant, so that mechanical variability between individual reeds is also much smaller. Nevertheless, some degree of variability may exist. Also, the mounting of the reed on the mouthpiece and the exact placement of the lip can slightly vary. Therefore, some tests will be repeated on different specimens. For the sake of conciseness not all measurements can be shown, but for relevant figures the result of a repeat measurement will be added so the reader can judge the degree of repeatability. To reduce effects of reed variability, the present study will use Légère Signature synthetic reeds produced by the Légère company (Légère Reed Ltd., Barrie, Ontario, Canada), one of the leading manufacturers.

Previous studies have investigated natural frequencies of the clarinet reed using digital holographic interferometry (Pinard et al., 2003; Taillard et al., 2014). In both publications, single-axis digital holography was used to measure the vibrational patterns along the axis perpendicular to the rest position of the reed. In the paper by (Pinard et al., 2003) clarinet reeds were mounted on a mouthpiece and reeds were stimulated acoustically to determine their natural modes. In the paper by

(Taillard et al., 2014), the reed was also stimulated acoustically and could move fully freely, hence the natural vibration modes of the free vibrating reed could be measured.

Opinions are divided on the link between the natural modes and the properties of the instrument's sound. In one paper (Taillard et al., 2014) it is suggested that the higher modes of the reed probably do not play an important role in the acoustics of the instrument, whereas another paper (Pinard et al., 2003) concludes that the musical quality of a reed can easily be assessed from the first three or four vibrational modes of the reed.

Although the study of reed vibrational modes gives important insight in the vibroacoustic behavior, it remains unclear how the reed vibrates in natural playing conditions and how it is influenced by the lip force and the shape of the mouthpiece. The frequency at which the reed starts to vibrate depends on the reed's own natural frequencies, lip force, mouthpiece shape and the natural frequencies of the air column to which the reed is connected (Benade and Gans, 1968). Depending on the tone hole configuration (which can be changed by opening and closing different tone holes) different acoustical properties are obtained in the instrument bore (Nederveen, 1969).

To develop a better understanding of the functioning of the reed and mouthpiece, the reed motion of the clarinet was studied by (Backus, 1961) with a photoelectric method using an artificial blowing machine. He showed reed vibrations for different notes. The results were only presented in a qualitative way so that no values are available for the displacement signal. (Colinot et al., 2020) studied alto saxophone reed vibrations using a single point optical probe in fully realistic playing conditions and defined several oscillation regimes. With the mouthpiece placed in the mouth, it is obviously impossible to measure reed vibrations over the entire surface, and conclusions need to be drawn on basis of single point measurements. The authors demonstrated that several oscillation regimes exist: during a note period, the reed can move to the mouthpiece once (single two-step regime) or twice (double two-step regime). If for some notes (e.g. in the higher playing register) the reed would be vibrating at a higher vibrational mode, as was the case in studies using external stimulation on free vibrating reeds, the amplitude at a single measurement point could be very different from the amplitude at other nearby points and give a poor representation of the overall motion of the reed. To verify if such higher vibration modes are of importance, measurements of 3D vibration patterns under realistic circumstances are needed.

(Picart et al., 2007, 2010) presented a testing method (digital Fresnel holography) for the measurement of reed vibrations over the entire visible surface and demonstrated the method with a measurement taken on a clarinet reed for a single note and lip force. The paper mentions the necessity to test reeds in different realistic playing conditions.

The shape of the mouthpiece has an important influence on instrument sound. Different mouthpiece designs exist for the clarinet, but for the saxophone the range of shapes is even more broad. Progress is being made in acoustical modeling of saxophone mouthpieces taking into account complex mouthpiece geometry information (Wang et al., 2021). Especially in mouthpieces aimed at jazz music, where an even broader range of pitch bending and loudness variation is preferred, a broad variety of geometries is being used in different music styles. Therefore, this work will focus on alto saxophone reeds mounted on two mouthpieces of different geometry. To analyze the motion of the reed, a previously developed setup is used. The measuring method is based on constant phase stroboscopic digital image correlation using high resolution cameras (see section II.C). Details on the setup and the measuring technique have been described earlier (Ukshini and Dirckx, 2021).
The reeds are mounted on a mouthpiece coupled to the instrument and driven by airflow between reed and mouthpiece, just like in the natural playing situation. The reed is bent and damped by a visco-elastic artificial lip (section II.B) with adjustable lip force. 3D vibration patterns are shown for

a number of different musical notes over the instrument playing range, different mouthpieces and under different lip forces.

The alto saxophone is a transposing instrument, meaning that the written note name differs from the note name in concert pitch. For the alto saxophone, the written note F# corresponds to concert note A. In all that follows, note names will be given in concert pitch.

In the present paper, the following research questions will be investigated:

- How does the reed vibrate under airflow-induced auto-oscillation, in presence of lip force, mouthpiece and instrument?
- Does mouthpiece geometry influence the 3D vibration patterns of the reed?
- Does the reed close against the mouthpiece only at the tip or also at the rest of its circumference?
- Do single point measurements give a correct representation for the overall (3D) motion of the reed?

The paper is structured as follows. Section II describes the materials and the measurement setup (details are given in (Ukshini and Dirckx, 2021)). In section III the results are presented for a single point (III.A), in three dimensions (III.B) and along selected cross sections (III.C). Because of the large amount of gathered data, only samples recorded at several notes and settings are shown in the paper. Full data sets, and 3D animations of reed motion are available online. Results are discussed in section IV and conclusions are drawn in section V.

II. MATERIALS AND METHODS

A. Mouthpiece and reed choice

For this study, two different mouthpieces (Concept and Spirit alto saxophone mouthpiece, Henri Selmer Paris) are used on an alto saxophone. The 'Concept' mouthpiece has a tip opening of 1.47mm and table length of 24 mm and is mainly intended to play classical music. The 'Spirit' mouthpiece has a larger tip opening of 2.1mm and table length of 27 mm and is aimed for jazz musicians. For the reed, new synthetic alto saxophone reeds made of polyethylene fibers (Légère Reed Ltd., Barrie, Ontario, Canada) are used. The use of synthetic reeds from the Signature series of Légère avoids variability between specimens and problems with humidification. The strength of the reed is 2 ¾ which is a commonly used average strength. To investigate the behavior in different musical registers, measurements were performed at the notes F3, A3, C4, F4, A4, C5 and F5. Tone holes were held with elastic bands to produce the appropriate note.

B. Experimental apparatus

Figure 1 shows a schematic representation of the experimental setup in top view. The saxophone is mounted on a metal support and part of the neck and the mouthpiece are placed in a transparent sealed pressurized container with dimensions of 20 by 20 centimeters. For practical reasons, the mouthpiece is turned over 180 degrees in comparison to the usual playing condition, so that the reed faces the camera. The cameras are at the level of the mouthpiece tip. Other views and more details on the setup can be found in (Ukshini and Dirckx, 2021).

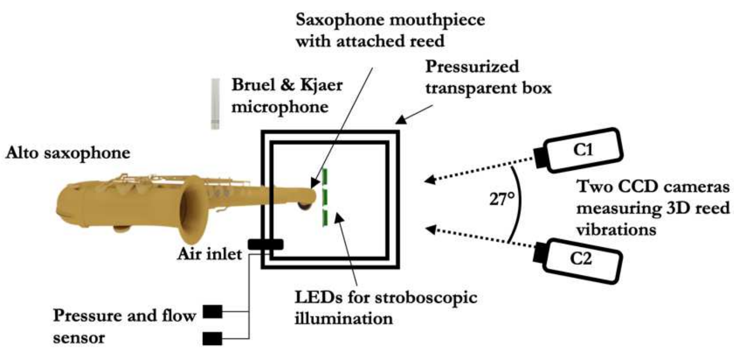

Figure 1: Top view schematic representation of the measurement setup. Two cameras (C1 & C2) observe the reed motion. The mouthpiece is positioned inside a pressurized transparent box and is turned in such a way that the reed faces the cameras. (color online)

A free field microphone (Bruel and Kjaer Type 2669, Denmark) is placed in the vicinity of the instrument to record the sound spectrum. An artificial lip was designed based on the average lip contact area of different players. The lip is made from a silicon resin with a Shore value of approximately 0. The amount of force exerted on the lip is measured with a loadcell (Honeywell FSS 1500NSR) and is controlled by the same computer that regulates air pressure and acquires sound signals and DIC images.

Air pressure is measured with a SCX 01 transducer (SenSym ICT) inside the pressurized box and airflow is measured with a flow sensor (Honeywell AWM720P1). Air pressure is computer controlled and can be set from 0 to 10 kPa, which covers the normal playing range of the saxophone (Fuks and Sundberg, 1999). Because the saxophone is designed to operate at the air temperature exhaled by the player, air temperature is maintained at 35 $\pm$ 0.5°C independent of the airflow through the instrument.

C. 3D DIC and coordinate system

Stereo digital Image Correlation (DIC) is used to obtain the full 3D motion of the reed over the visible surface of the reed. In DIC, the images are subdivided in a number of facets consisting of for instance 40 by 40 pixels. The gray scale information of each facet in the image of one camera is then correlated to the corresponding facet in the image of the other camera. After calibration, this method allows to calculate the position of each facet in 3D space. Because the entire gray scale distribution is used, the average in-plane position of the facet can be determined with a subpixel precision of typically 0.1 image pixel. To be able to use gray scale information and in order to have a unique solution in the correlation process, the object surface needs to have some random optical texture (Pan et al., 2010). A commonly used technique to obtain such texture is by spraying a fine ink speckle pattern onto the object surface. Since the Légère reeds are transparent, the background in the images is dark due to the black color of the mouthpieces. Therefore, a white speckle pattern is sprayed on the reed utilizing an aerosol with white ink. Before starting a measurement, a calibration of the DIC system is performed using a calibration plate. Because the displacements of the reed are of order tenths of a mm (Bucur, 2019), DIC is a highly suitable technique to study the reed motion. More details on the DIC technique can be found in (Pan et al., 2009; Sutton et al., 2009).

For the sake of clarity, Figure 2 defines a coordinate system in which all the data is presented. The origin of the x-axis is set at the middle of the mouthpiece tip and the z-axis is chosen perpendicular

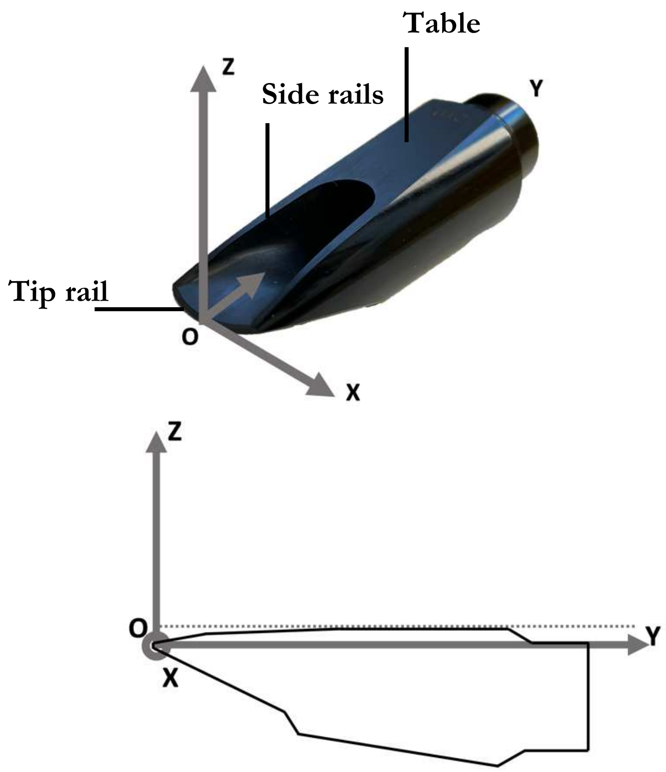

Figure 2: Coordinate system in which the data is presented in. The origin of the x-axis is set at the middle of the mouthpiece tip. The z-axis is chosen perpendicular to the surface of the mouthpiece table, with its origin at the level of the mouthpiece tip. The dotted line indicates the level of the mouthpiece table. (color online)

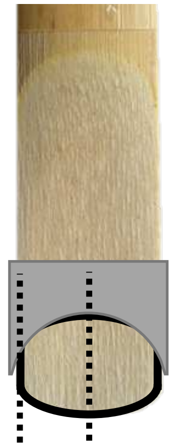

Figure 3: Top view on a reed with the artificial lip in place. The black line indicates the circumference of the zone in which 3D vibration data are measured. The dotted lines indicate the locations of cross sections along which reed motion will be shown (Section III.C). The artificial lip is indicated with gray. (color online)

In Figure 3 the position of the artificial lip is shown, and the boundary of the visible reed surface, on which 3D vibration data is presented, is indicated in a black line. The dotted lines indicate the position along which cross section data is presented (Section III.C, Fig. 14).

D. Reed dynamic motion

To examine the dynamic 3D reed vibrations, stereoscopic DIC was combined with a stroboscopic illumination technique based on a delay triggering system. A Q400 3D digital image correlation system with commercially available software (ISTRA 4D 4.4.7, Dantec Dynamics, Skovlunde, Denmark) was used to capture and correlate the recorded stereoscopic images. Two Manta G609B cameras (Allied Vision Technologies, GmbH, Stadtroda, Germany) with a resolution of 2056x2464 pixels were placed under and an angle of 13.5° to the left and to the right of the normal on the reed plane, which is good suitable angle to capture the out of plane displacement (Reu, 2013). For the evaluation of the DIC results, the facet and grid size were set respectively 39 and 29 pixels. The distance between two data points on the reed is $210\mu m$. The stereoscopic DIC technique allows to measure three dimensional motions on a dense grid of points on an object surface, with a measuring precision up to 0.1 pixels for in-plane motions (Bornert et al., 2012; Reu et al., 2015). For the out-of-plane motions (which are by far the largest component in the motion of the reed), the measuring precision is a factor 2-3 less good (Balcaen et al., 2017). In a separate experiment[1] the out-of-plane measurement uncertainty for the current setup was found to be better than 2μm for all displacement measurements.

The inlet blowing pressure (pressure in the box containing the mouthpiece) is adjusted to obtain stable oscillation. The signals of the pressure and lip transducer were recorded in ISTRA 4D simultaneously with the captured images. In the dynamic regime, the periodic motion of the reed is an auto-oscillation generated by the physics of the musical instrument and the airflow-reed-mouthpiece combination.

To sample the reed's vibration cycle, the oscillation frequency is first determined from the measured sound spectrum. The zero-passing of the sound signal is used to trigger image acquisition. Because the motion of the reed is highly non-sinusoidal, a programmable bandpass filter is used to filter the fundamental frequency out of the sound signal before the signal is passed on to the zero-crossing detector. This assured that the high-power LEDs used for the stroboscopic illumination are not triggered incorrectly by a zero-passing different from the fundamental frequency. Finally, the LED light stroboscopic pulses are fired at a computer-controlled time delay after this zero passing (corresponding to the desired phase in the vibration period). The light pulses are integrated over the shutter time to gather enough light for the correlation of the data. The duty cycle of the LEDs was set to 1% of the reed vibration period, and images were acquired at 20 equidistant time steps. The reed vibration cycle was sampled in 20 subsequent steps equally divided over the vibration cycle. From the 20 acquired images the full periodic motion of the reed could be reconstructed over the entire visible surface of the reed. In accordance with the Nyquist theorem, sampling the periodic motion in such a way allows an analysis up to the ninth harmonic.

The DIC technique measures the location of the upper surface of the reed. To make interpretation easier, the thickness of the reed is subtracted from the DIC data, so that the motion of the reed backplane is shown (section III, Figures 4,6,7,8,14). In this way, the closing of the reed against the mouthpiece can be easily seen.

III. RESULTS

A. Single point analysis of reed periodic motion

1. Single two-step motion and repeatability

Figure 4 shows the periodic motion at A4 for a point in the middle of the reed tip close to the rim, for three different lip forces and with the reed mounted on the Concept mouthpiece. For each lip force the measurement is repeated using three new Légère Reeds. Repeat measurements for each lip force are indicated using the same marker and color line. Due to the mechanical limitations of the lip translation setup, the actual measured lip force deviates slightly from the set lip force (5%).

The blowing pressure is set to a constant value of 4 kPa. This value is in the middle of the blowing pressures measured for the alto saxophone (Fuks and Sundberg, 1999).

The behavior of position as function of time is very similar for the three different reeds. For all lip forces, the variability of the peak-to-peak amplitude over the three reeds is less than 10%.

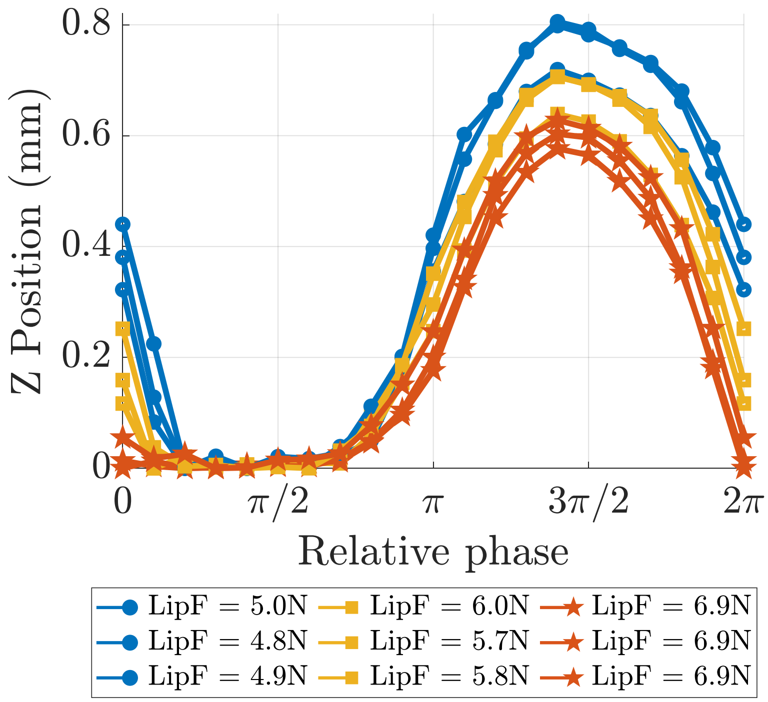

Figure 4: Position of the backside of the reed tip center as a function of time measured at note A4 for three different lip forces on a reed mounted on the Concept mouthpiece. Measurements are repeated using three different reeds with the same nominal strength. Repeat measurements are indicated using the same markers and line colors. (color online)

On this note, the simple two-step vibration regime is observed (Colinot et al., 2020), and the reed comes very close to the mouthpiece tip for about one third of the vibration period. For the different lip forces, the overall motion of the reed is similar, yet the amplitude differs. For the lowest lip force, the reed opening can be as high as 0.79mm. The maximum opening for the highest lip force is 0.62mm. The lip influences the maximum deflection of the reed relative to the mouthpiece. In the closing part of the vibration cycle, the reed does not remain in contact with the mouthpiece. A bounce effect of 22 μm is observed for a lip force applied of 4.9N. The bounce effect is seen in more detail in Figure 8 (section III.A.4.)

Figure 5(a) shows the corresponding spectrum of the vibration cycle shown in Figure 4. The fundamental frequency and the first six harmonics of the displacement signal are represented. Higher harmonics are not shown because the corresponding values were not always above the noise level. The amplitude is plotted on a logarithmic scale to better visualize the higher harmonics. In contrary to all other figures, the spectrum is calculated for the reed displacement relative to the reed's resting position with lip force applied but without airflow. In this way, the DC component indicates the change of equilibrium position caused by the airflow.

The DC displacement of the reed (induced by air flow) is seen as the first peak at zero, and it is about as high as the amplitude at the fundamental vibration frequency. The frequency at which the reed oscillated was respectively 440Hz at 4.9N, 441Hz at 5.8N and 442Hz at 6.9N. The frequency of the reed's vibration is slightly increased by adding more lip force. The DC component of the Fourier spectrum with $F_{lip,mean}$= 4.9N is 0.44mm meaning the reed's oscillation is occurring around 0.44mm lower than rest position (with lip force applied). The DC offset value for $F_{lip,mean}$= 5.8N and $F_{lip,mean}$= 6.9N are respectively 0.41mm and 0.39mm. Figure 5 shows that the strongest frequency component of the reed motion is at the fundamental frequency, with an amplitude of at least a factor of four higher at the middle than the amplitude at the first harmonic. The harmonics of the signal are much lower in amplitude as compared to the fundamental frequency. For the first three harmonics, amplitudes above 5% of the amplitude of the fundamental are observed. The fourth until the sixth harmonic all show relative amplitudes below 5%.

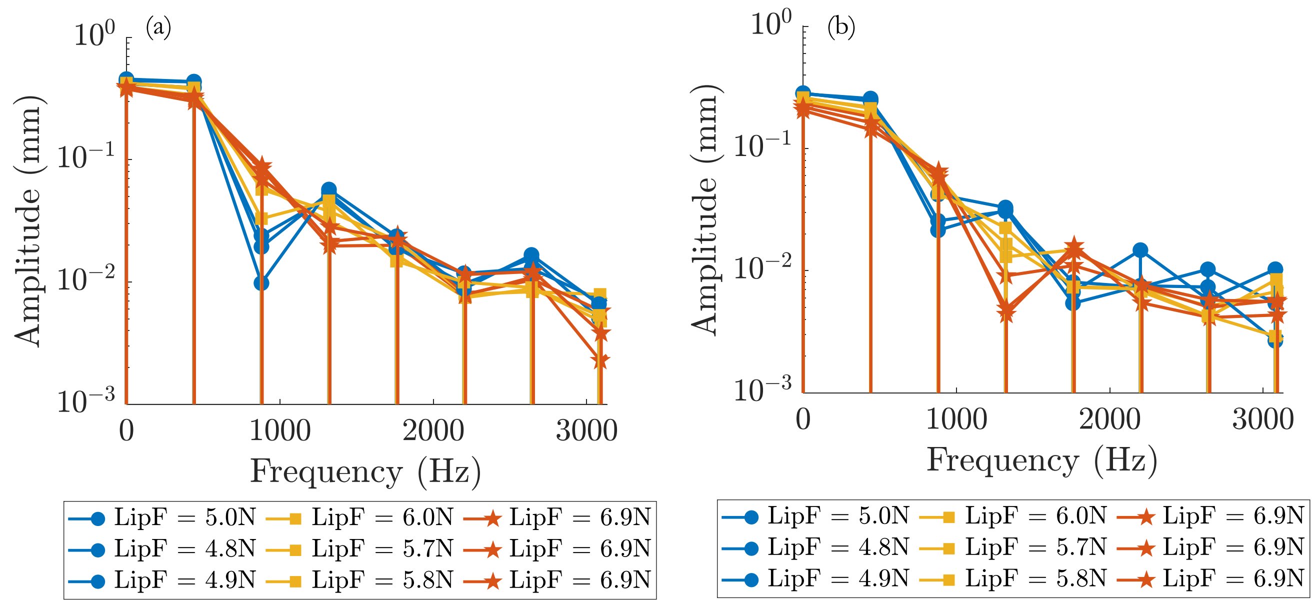

Figure 5: Frequency spectra for A4 measured at (a) the vicinity of the reed tip and (b) bottom left side of the reed. The fundamental and the first six harmonics are shown. Different markers are used to show the different lip forces. Repeat measurements with different reeds are indicated by the same markers. The DC component is shown as well. (color online)

Figure 5(b) shows the spectrum for a left bottom point at the reed's surface near the side rails of the mouthpiece. Generally, the amplitude of the spectrum is lower as compared to the amplitude spectrum obtained at the center of the reed tip. The relative strength of the first harmonic is larger near the side rails than in the middle. Different lip forces mainly influence the relative amplitudes of the harmonics. For all lip forces, the spectra obtained for three different reed samples are very similar.

2. Double two-step motion

Figure 6 shows the periodic motion at F3 as a function of relative phase, for 20 subsequent phase steps measured over one period. The motion is shown for a point in the middle of the reed at the vicinity of the tip with the reed mounted on the Concept mouthpiece. During one oscillation, the reed moves multiple times towards and away from the mouthpiece. At this note, the double two-step behavior is seen, as described earlier (Colinot et al., 2020) on the alto saxophone under realistic playing conditions. A negative slope of the curve means the reed moves towards the mouthpiece. The pressure at which stable dynamic motion was initiated is 3.4 kPa for the highest lip force and 2.4 kPa for the lowest lip force. The maximum deflection of the reed from the mouthpiece tip is 0.91 mm (third point on the vibration cycle). At this phase, the reed is furthest from the mouthpiece. Next, the opening between the reed and the mouthpiece becomes smaller and nearly fully closes, leaving a gap of less than 30 μm. Afterwards the reed moves away from the mouthpiece tip and the reed channel becomes again 0.91mm and finally the reed closes against the mouthpiece for a second time within the same vibration period. The vibration amplitude again depends on lip force. For F_{Lip}=6.9N the maximum amplitude is 0.53mm.

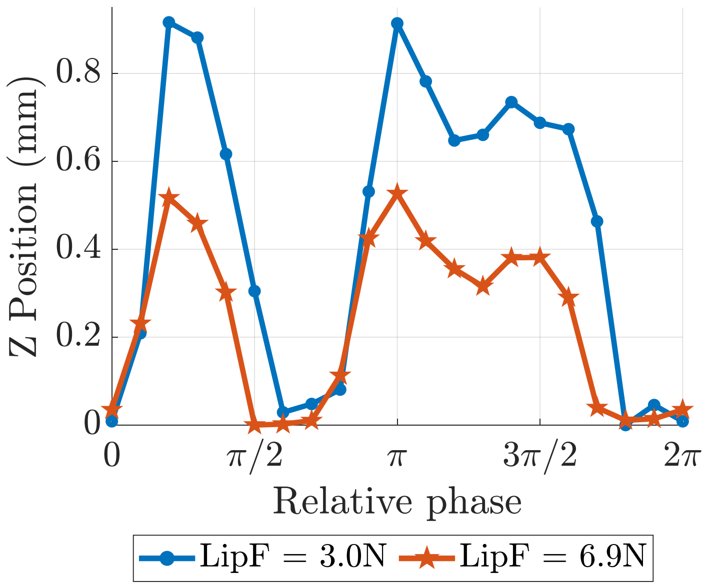

Figure 6: Position of the backside of the reed tip center as a function of time measured at note F3 for two different lip forces on a reed mounted on the Concept mouthpiece. The markers indicate the measured time steps. The double two-step vibration regime is seen. (color online)

3. Influence of mouthpiece on reed periodic motion

A direct comparison between the two mouthpieces could not be performed because the different mouthpieces required a different minimal lip force to initiate auto-oscillation of the reed. Therefore, the influence of the two different mouthpieces on the motion of the reed is analyzed using different lip forces. Figure 7 shows the vibration cycle at A4 for the different mouthpieces and different lip forces. The reed motion on the Spirit mouthpiece is clearly different from the motion on the Concept mouthpiece: when the reed is attached to the jazz mouthpiece, the reed remains open during a longer part of its periodic motion.

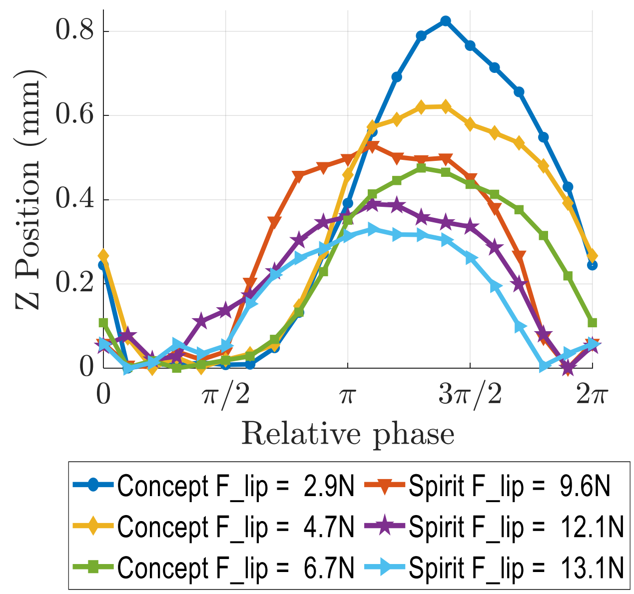

Figure 7: Position of the reed bottom for different lip forces and different mouthpieces measured at note A4. When the reed is attached to the Concept mouthpiece the reed gap remains closed for a longer fraction of the vibration period than when the reed is mounted on the Spirit mouthpiece. (color online)

To initiate auto-oscillation with the reed attached to the jazz mouthpiece, the reed is initially more bent by the applied lip force. A minimal lip force of 9.6N is needed whereas for the Concept mouthpiece the lip force can be more than a factor three lower to start the reed vibrating. The amplitude of the reed motion on the Spirit mouthpiece is smaller than 0.6mm for all tested lip forces, while for the Concept mouthpiece the amplitude reaches 0.8mm. When using the same reed strength, higher lip forces are needed to obtain oscillation on the Spirit mouthpiece. When lip force is changed over a similar range of about 3N, the change in vibration amplitude is considerably larger on the Concept mouthpiece (0.35mm) compared to the Spirit mouthpiece (0.2mm). The figure demonstrates that mouthpiece geometry has an important influence on reed motion as function of time.

4. Bounce effect

Figure 8 shows the position of a point at the center of the reed tip (near the edge) as a function of time, for 20 subsequent phase steps measured over one period of C5. The circles and triangles indicate the subsequent measured time steps (different symbols and gray scales were used corresponding to cross-section profiles which will be shown in Figure 14). The peak-to-peak amplitude of the tip vibration is 0.77 mm. For more than a quarter of the vibration period, the reed tip is practically in contact with the mouthpiece, although at some time points a re-opening with an amplitude of 40µm occurs.

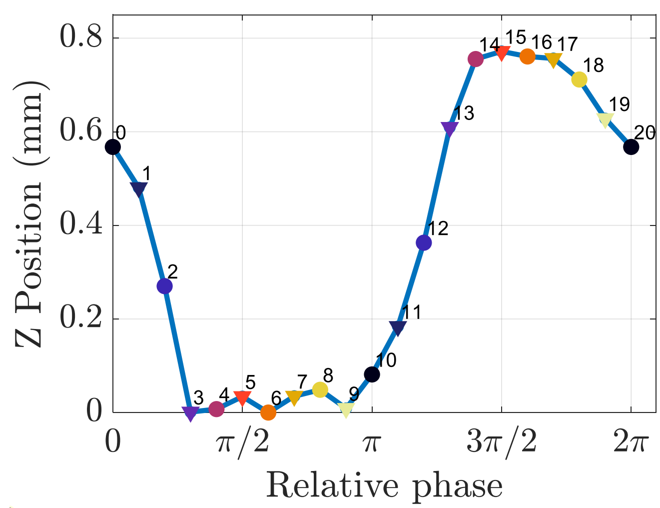

Figure 8: Position of the backside of the reed tip center as a function of vibration phase measured at note C5. Dots and triangles indicate the time steps at which measurements were made (subsequent gray values and symbols correspond to reed cross sections shown in Figure 14) and are labeled from 0 to 20. Each subsequent time step number corresponds to a phase increase of 2π/20. The reed tip nearly touches the mouthpiece for more than a quarter of the vibration period. (color online)

B. 3D reed motion

1. Magnitude maps of reeds mounted on a Concept mouthpiece

Section III.A showed the vibration cycle for single points on the reed's surface. DIC provides displacement maps over the whole visible surface of the reed at all measured time steps, which results in a substantial amount of data. Instead of presenting the displacement maps for each measured time step, the maximum measured magnitude map and its decomposition on the fundamental frequency and harmonics are shown. Full field animations of reed motion can be found in the supplementary material.[2]

To calculate the frequency decomposed magnitude maps, the out of plane displacement is stored in a 2D matrix where each point in the matrix represents a position on the reed's surface. Next, a 3D matrix is constructed by adding the data of the out of plane displacement of each sampled time step. Afterwards, the Fourier spectra of the displacement signal are calculated in each point of the matrix. Only the first six harmonics are shown because for higher harmonics the magnitudes become too low to surpass the 2 micrometer sensitivity level of the DIC setup.

As an example, Figure 9 shows the measured magnitude maps and their decomposition on the note fundamental and the sixth upper harmonics for A4 played on the Concept mouthpiece for three different lip forces. The final column shows the full-field amplitude maps for a repeat measurement using a different reed and approximately the same lip force as used to obtain the data shown in the second column (Lip force ≈ 6N). For the sake of clarity, the magnitude is chosen different for each row because amplitudes strongly decrease for the higher harmonics. The magnitude scales at the harmonics are a factor 8, 8, 20, 20, 20 and 40 times smaller than the scale used for the fundamental frequency. The blowing pressure is 4 kPa for all the measurements. The measured magnitude distributions (top row of Figure 9) show that the reed mainly vibrates in its first flexural mode.

Increasing lip force leads to smaller vibration amplitudes, but overall the shape of the magnitude map remains the same. Decomposing the magnitude map onto the note fundamental and its harmonics reveals more detail. For all lip forces, the amplitudes at f_0 are at least a factor of 3.5 higher than the amplitudes of any of the harmonics. For the lowest lip force, the magnitude at the first harmonic at a point in the middle of the reed tip is more than 20 times smaller than the magnitude at f_0. For harmonics beyond f_3, all magnitudes are more than 20 times smaller than the magnitude at f_0. Increasing lip force results in lower amplitudes, as was already shown for a single point in section III.A.1. At f_0 the maximum magnitude at the lowest lip force is 0.44mm at the tip of the reed (decreasing to 0.24mm at 5mm from the tip). For the highest lip force, the maximum magnitude is 0.32mm, or a factor of 1.4 lower as compared to the value obtained at the lowest lip force. At the harmonics, lip force also influences the shape of the magnitude maps. At f_1 the lowest lip force shows a different map than at the higher lip forces, and for f_6 the different lip forces yield very different magnitude maps. Apart from that, the shape of all magnitude maps is rather similar for the different lip forces.

The right most column of Figure 9 shows the repeat measurement with a different reed, for approximately the same lip force settings as used for the second column of the figure. A very similar result was obtained for a third reed. Both for the fundamental as well as for all harmonics, the magnitude patterns are largely the same, but some subtle differences can be seen. At f_4 the amplitude at the side tips of the reed is markedly larger in the first measurement than in the repeat measurement. Especially at f_6 the vibration patterns differ: for both reeds the magnitude map corresponds to a torsional mode of the reed, but amplitudes at center and side tips are markedly different.

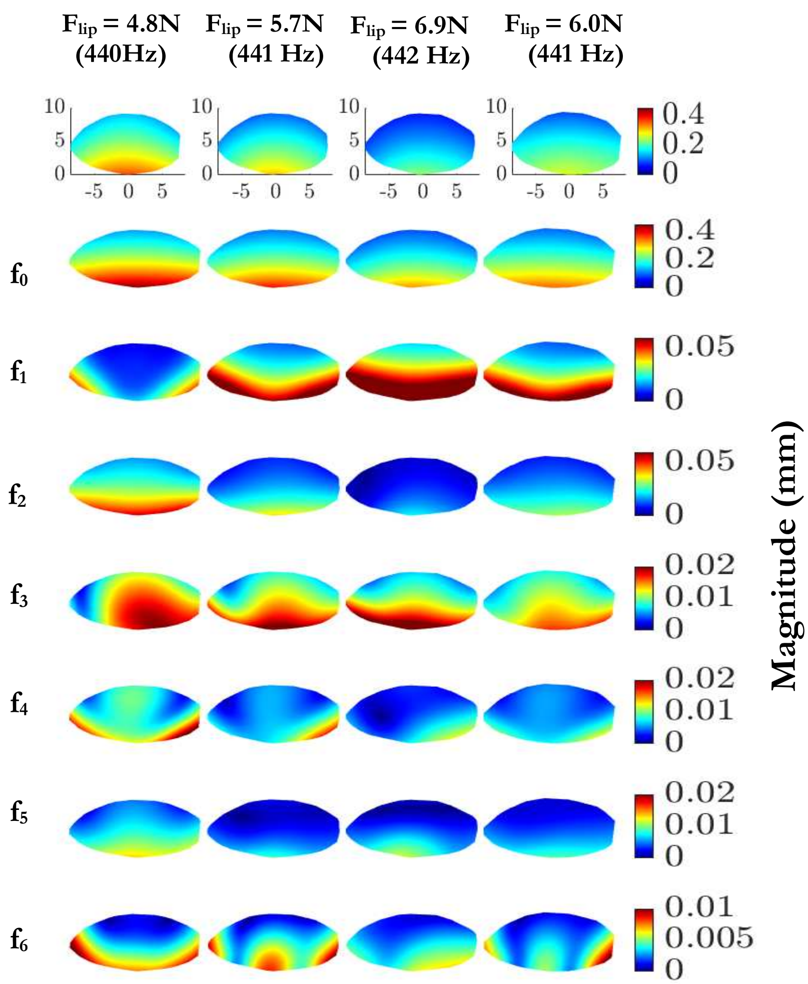

Figure 9: Measured magnitude maps (first row) and their decomposition on the fundamental and first six harmonic components for the reed vibrating at A4 on a Concept mouthpiece with different lip forces applied. The simple up-and-down movement of the first fundamental is by far the most important component in the motion, but higher vibration modes are also present and differ in relative amplitude depending on lip force. The most right column shows a repeat measurement on a different reed using approximately the same reed force as used for the data shown in the second column. (color online)

2. Effect of mouthpiece on reed vibrations

Figure 10 shows the measured magnitude maps, and their decomposition on the note fundamental and its harmonics, for the Concept and Sprit mouthpiece at the note C5. The jazz mouthpiece requires a higher lip force and different blowing pressure to initiate auto-oscillation, so care should be taken in comparing the results. The main observation is that for both mouthpieces the reed vibrates mainly in its first flexural mode again. For both mouthpieces amplitudes at the harmonics are at least a factor of 5 smaller than on the fundamental. On the jazz mouthpiece, the amplitude of the fourth harmonic is 66% higher than on the Concept mouthpiece. For both mouthpieces, existence of small amplitude higher vibration modes can be seen at different harmonics.

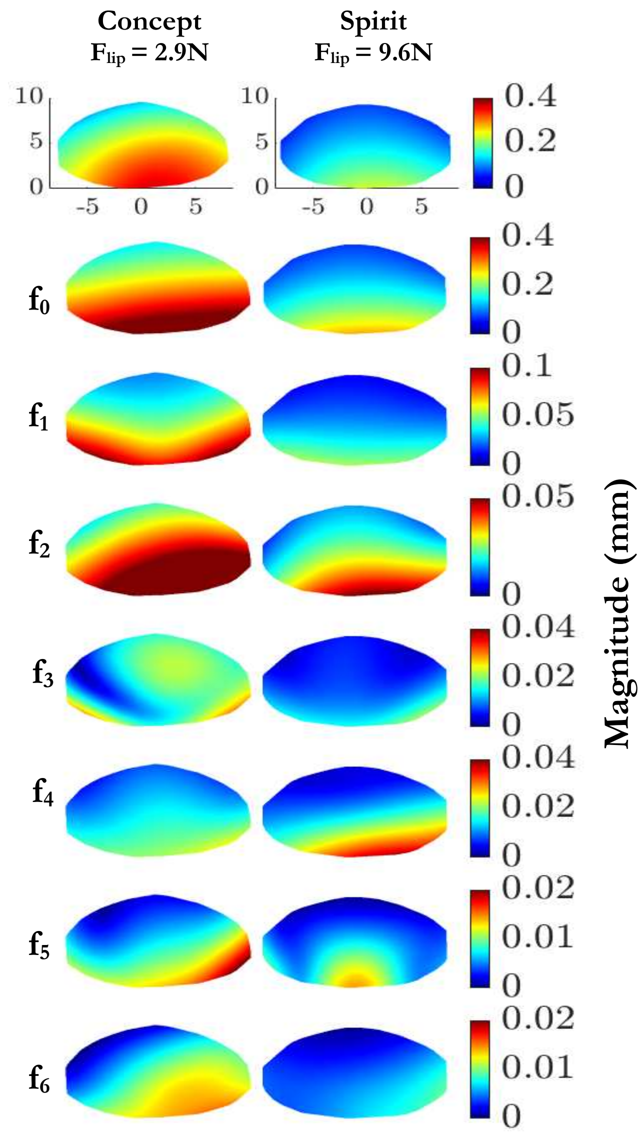

Figure 10: Measured magnitude maps (first row) and their decomposition on the fundamental and first six harmonic components for the reed vibrating at C5 on a Concept and Spirit mouthpiece. On the Spirit mouthpiece a higher lip force is needed, and vibration magnitude is smaller than on the Concept mouthpiece. The contribution at f_4 is however much higher on the Spirit mouthpiece. (color online)

3. Magnitude maps for different musical notes

Finally, Figure 11 shows an overview of the magnitude of the reed displacement obtained for the reed mounted on the Concept mouthpiece, for all the tested notes. A similar figure for the Spirit mouthpiece can be found online[3] (see supplementary material). Magnitudes are again calculated at the fundamental of the played note and at the first six harmonics of that note. For each fundamental, and for each mouthpiece, different color scales are used to be able to represent the values clearly. The figure shows that for all notes the reed vibrates in a simple up-and-down going motion up till at least the second harmonic. As of the third harmonic, more complex magnitude distribution patterns start to show up, especially in the higher notes. For the three lowest measured notes, which are notes of the first register of the saxophone, the maximum magnitudes for f_0 are respectively 0.17mm, 0.33mm and 0.34mm. For the notes F4, A4, C5, the maximum magnitudes are respectively 0.45, 0.44 and 0.46mm for f_0. For f_1 the maximum magnitudes of the second register notes (F4, A4, C5) are smaller (resp. 0.06mm, 0.07mm, 0.1mm) compared to the maximum magnitudes of the first register notes (resp. 0.32mm, 0.22mm, 0.24mm).

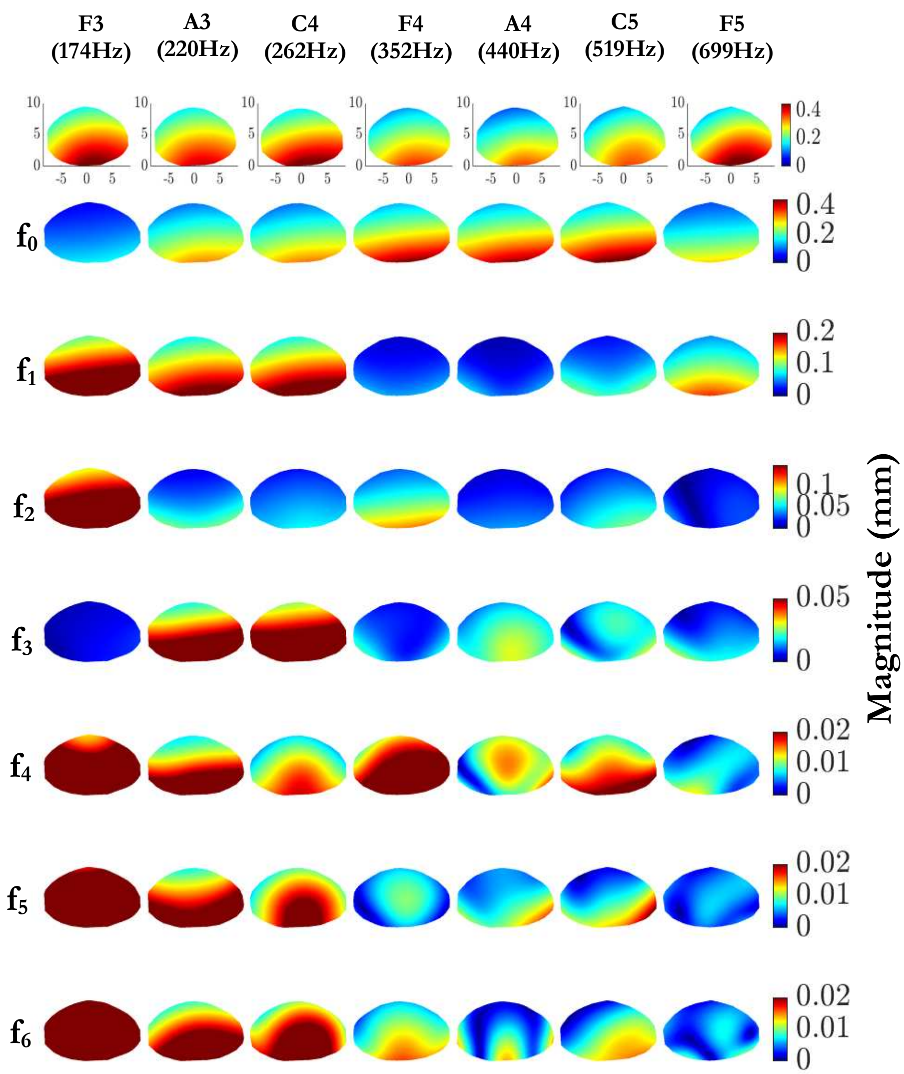

Figure 11: Measured magnitude maps (first row) and their decomposition on the fundamental and first six harmonic components, with the reed mounted on the Concept mouthpiece, with lip force applied of 2.9N. (color online)

4. 3D displacement maps as a function of time

As an example of the measured 3D motions a 3D animated representation of the movement of the reed vibrating on a Spirit mouthpiece at F5 can be seen in Mm.1.

Mm.1. Animation: 3D reed motion at F5 on a Spirit mouthpiece.

Even at this highest tested note, the reed is essentially still moving in first flexural mode. The amplitude of the higher modes is so small that they can better be seen by the harmonic decompositions shown in Figures 9,10,11.

In Mm.2, a 3D animation is also presented of the fraction of the motion taken at the 4^{th} harmonic of the played note.

Mm.2. Animation: 3D reed motion at fourth harmonic of F5 measured on a Spirit mouthpiece.

Obviously, a very different scale had to be used to be able to show this motion. The scale of the harmonic is 30 times smaller. This complex vibration pattern is superimposed on the vibration pattern at the fundamental, but its amplitude is so small that it can hardly be observed in the overall motion.

5. Operational modal analysis

In the previous section (III.B.), the measured vibration pattern was decomposed onto the harmonics of the produced musical note. Another way to analyze the data is to perform an operational modal analysis (OMA) (Brincker, 2015). The response of the structure (here the reed) due to the excitation by airflow may contain many vibrational modes. This modal representation allows to quantitatively evaluate the implication of the various modes (flexural/torsional) in the observed motion of the reed. The benefit of an OMA is that it does not require any controlled excitation. To estimate the modal parameters from OMA, the Frequency Domain Decomposition (FDD) method was used. In brief, the magnitude data over the whole visible surface of the reed of each harmonic component in the frequency domain is stored into a column of a matrix A. Next, a Singular Value Decomposition (SVD) of this large matrix A is performed so that A=USV' (Fadhil Shazmir et al., 2018) where U and V are unitary matrices with U holding the shape modes. S is a diagonal matrix holding the real and nonnegative singular values of A in descending order starting with the highest value at the upper left corner (Brincker, 2015). Each singular value corresponds to a column vector of U which represents a shape mode. Figure 12 shows the shape of these vibrational modes obtained for note C5 on the Concept and the Spirit mouthpiece. Their normalized singular values in both mouthpieces and for all notes are given in Figure 13 ((a) Concept, (b) Spirit). Figure 12 shows that for both mouthpieces, the first operational mode is the first bending mode. The higher operational modes have more complicated patterns. For the Concept mouthpiece, Figure 13(a) shows that the amplitude of the second vibrational mode is nearly a factor of 36 lower than the first mode.

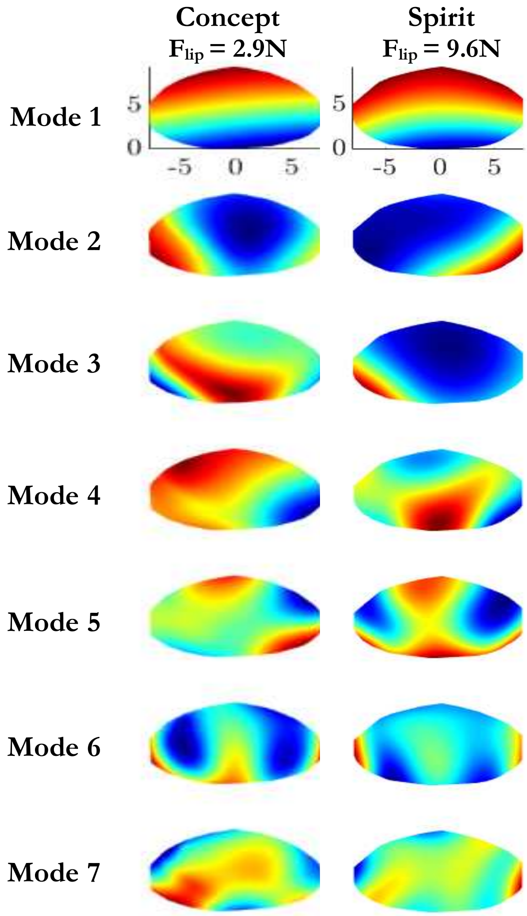

Figure 12: Shape of the first seven operational modes of the reed vibrating on the Concept (left column) and Spirit (right column) mouthpiece, for note C5. The grayscales (color online) only display the shape of the mode. On both mouthpieces, the first operational mode is the simple bending mode. The second mode is a torsional mode. Higher modes are more complicated. (color online)

453

For the Spirit mouthpiece, this factor is 39. In the supplementary material[4], the first seven operational shape modes are shown for all measured notes on both mouthpieces. In all cases, the

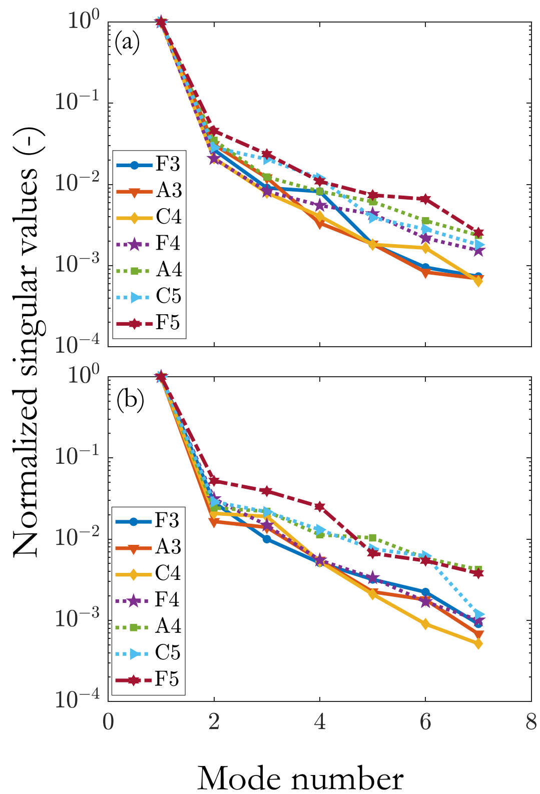

Figure 13: Relative contribution of the first seven operational modes for (a) Concept mouthpiece, (b) Spirit mouthpiece shown in Fig. 12. Results for notes in the lower register of the instrument are indicated by full lines, results for notes in the higher register are indicated by dashed lines. Because values decrease dramatically with mode number, results are shown on a logarithmic scale. The amplitude of the second mode is nearly 40 times smaller than the amplitude of the first mode. Values haven been normalized with respect to the value at the first mode. (color online)

first bending mode is clearly seen and by far the most dominant, being a factor of nearly 40 times larger than the next mode.

C. Cross-sectional views at centerline and near side rails

For subsequent time steps, the top row of Figure 14 shows the position of the back side of the reed along a vertical cross section taken near the side of the mouthpiece (see Figure 3). The bottom row shows the positions for a cross section at the center of the mouthpiece. Results at time steps in the first and second half of the vibration period are shown in the first and second column, respectively. The position of the start of the artificial lip is indicated by an arrow. As the lip is curved, the y-coordinate of this position is different for the two sections. As the tip of the reed is also curved, the position of the start of the section is also different between the top and bottom row panes of Figure 14. In each pane, the mouthpiece material, at the level position where the cross section was taken, is indicated in black. The projection of the entire mouthpiece on a plane parallel to the Y-Z plane is indicated in gray.

469

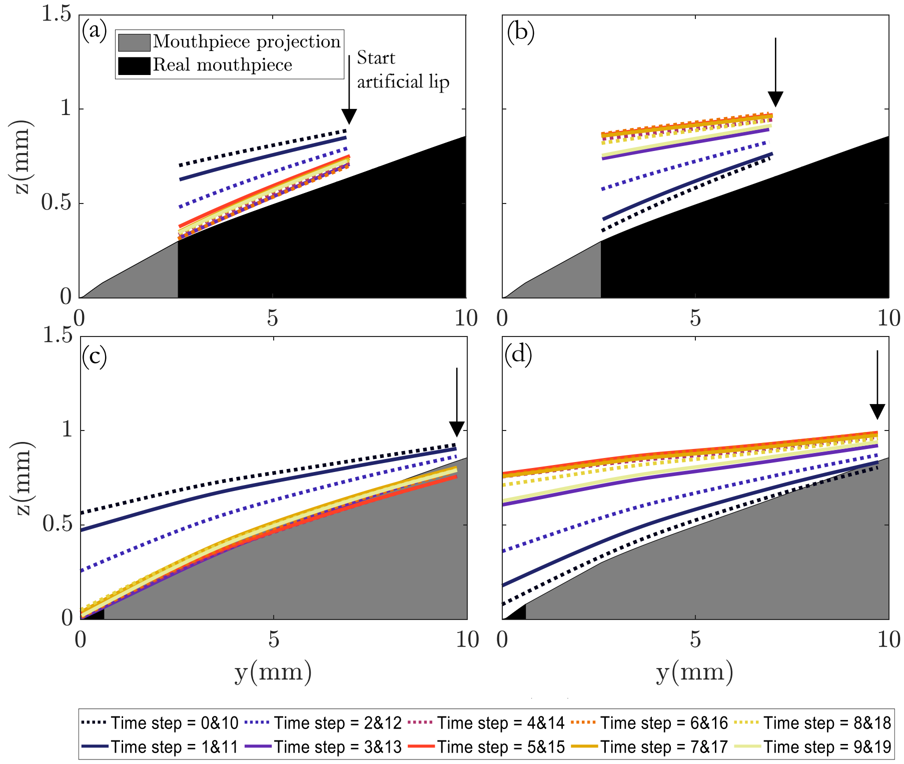

Figure 14: cross sections along the Y-axis of the back side of the reed, measured at the subsequent time steps indicated in Figure 8. Top row shows motion of the section taken at the side of the reed, bottom row shows motion of the section at the center of the reed (location of the section as indicated in Fig. 3). Left and right panel respectively show the first and second half of the vibration cycle. To better distinguish subsequent curves, data obtained at even time points are indicated with dashed lines and data at odd time points are indicated using full lines. The black zone indicates the mouthpiece material at the location of the section. The gray zone indicates the projection of the mouthpiece shape onto the Y-Z plane. The position of the start of the lip is indicated by arrows. (color online)

To obtain the cross sections at the backplane of the reed, the reed thickness profile is subtracted. This reed thickness profile is obtained from a separate DIC measurement in which the reed is placed on a flat reference surface. The DIC measurement accuracy on the line profiles near the edge is less good than on smooth surfaces, and the thickness is obtained from a separate DIC measurement, reducing the measurement accuracy to about 15 micrometers in the reference frame of the mouthpiece. Each cross section corresponds to a subsequent time step: to better distinguish between the different profiles, different gray values and line shapes have been used, as defined in the legend of the figure (color online). It is important to notice that to better visualize details, the Z-axis has been expanded with a factor of 5 with respect to the Y-axis.

At the front the reed almost completely closes against the mouthpiece. The gap is less than 15 μm. Along the visible part of the reed, the gap slightly increases to a value of about 50 μm at the position y=7mm for the lowest cross-section position in the first half part of the vibration period.

Figure 14(c) and (d) show the position of the back plane of the reed for a cross section along the Y-axis taken in the center. Different gray values and line shapes are again used to indicate profiles measured at subsequent time steps. At time step 3 the reed touches the mouthpiece. For several time steps the back side of the reed is lower than the position of the side rails of the mouthpiece. For time step 5 (when the bounce effect occurs) the reed's back side profile at y=9mm lies 70 μm below the level of the facings of the mouthpiece.

IV. DISCUSSION

A. Methodology

1. Lip design

The results shown in this paper were acquired with a custom-developed artificial lip. The lip has a significant influence on the reed motion. When a lip is made from a material with a higher stiffness, the lip force can be smaller to initiate auto-oscillation of the reed, but the produced sound is affected as well. Moreover, the lip needs to be useful over the different registers of the saxophone. In a previous paper, little information was found about the lip design and its material parameters (Kobata and Idogawa, 1993). (Almeida et al., 2013) used a lip of polyurethane foam with a rectangular geometry. In this work, the lip design was based on lip prints taken from experienced players to determine the contact zone of the lip on the reed. Based on these prints the lip had a semi-circular ending and was placed at approximately 10 mm from the reed rim. On basis of qualitative preparatory experiments, a silicone material with hardness Shore A$\approx$ 0 was used which was found to be in the same stiffness range as a natural lip. For the present study it was sufficient to use a lip which allows to set the reed into vibration over a broad range of notes and with physiologically acceptable lip forces and blowing pressures. The lip design produced comfortably the musical notes over a broad playing range. The applied lip forces in the experiment are in the range of 2-7N on the Concept mouthpiece and 10-13N on the Spirit mouthpiece. Other authors have reported lip forces in the range of 1-7N for the clarinet (Mayer, 2003), using a Plasticover reed with strength 5, but specifications of the lip are not mentioned in the paper. As the influence of the lip is clearly important, further systematic investigation of lip shape and material parameters will be most relevant, but this is beyond the scope of the present paper.

2. Repeatability

Figure 4 showed the motion of the center of the tip of the reed as a function of time, for three different new reeds. The three measurement results are very similar, and the difference in peak-to-peak amplitude is less than 10%. The final column of Figure 9 showed a repeat measurement of full-field vibration amplitude for a different reed under the same circumstances as the sample presented in the first column. The overall amplitude distribution, and the amplitude distribution at the lower harmonics (until f_2) is very similar. At the higher harmonics, repeatability is less good. Similar results were obtained for a third reed. As a whole, the repeatability measurements show that vibration amplitudes differ only little between different reed samples, but small effects of shape and mounting do have an influence on the low-amplitude higher harmonics. (Gazengel et al., 2016) found far larger variability in natural cane reeds. In such reeds, the density and orientation of fibers, and hence the mechanical characteristics, can differ rather strongly from one sample to the next, even though the external profile of the reeds is milled into the same shape to a very high precision. For the synthetic reeds, differences in mechanical behavior are caused only by tolerances in the milling process of the reed shape, as mechanical parameters of the synthetic materials can be expected to be nearly identical over all samples.

3. Reed excitation

The blowing pressure is actively regulated by a PID feedback circuit using proportional valves, but it can still slightly change over time. This and other mechanical variations may lead to small changes of the reed vibration frequency, which in turn could result in some blurring of the phase at which measurements are obtained within the vibration period. The acquisition of the 20 phase steps takes about 50 s in total. A laser vibrometer was used to constantly measure the full vibration signal at one point of the reed. The Fourier spectrum of this measurement showed that the deviation of the vibration frequency over a period of 50 seconds is less than 0.25%, so phase blurring is also smaller than this number.

In experiments using acoustic stimulation, the input pressure driving the reed is well defined, and the input/output relationship between pressure and reed motion can be precisely determined. In the current experiments the driving pressure is not known; it is the result of the aerodynamic properties of the mouthpiece, the acoustic properties of the mouthpiece and the instrument, and of the reed motion itself. Therefore, no conclusions can yet be drawn as to the relationship between the motion of the reed and the driving pressure.

4. Data analysis

The DIC measurements are performed on 20 phase steps, so according to the Nyquist criterion, undersampling artifacts can occur if the reed vibration contains frequency components starting from 10 times the fundamental frequency. The duty cycle of the LED illumination is set to 1% of the vibration period, and motion of the reed within this time frame is integrated on the camera sensor. This integration functions as an analog low-pass filtering (much the same as a low-pass filter preceding an A/D converter), so that no higher frequencies than 200 times the fundamental vibration frequency can enter the system. This however still leaves a gap between the analog low-pass filtering cut-off and the highest frequency that can be reliably measured at 20 samples per period. In a preparatory investigation it was checked that no undersampling artifacts were recorded. A single point laser vibrometer (Ukshini and Dirckx, 2021) was used to check the entire spectral content of reed vibration on several points, using a sampling frequency of 100ks/s. These measurements showed that for frequencies 10 times the fundamental and beyond, amplitudes are far smaller than what can be detected by the DIC system, so they cannot influence the amplitudes calculated at the lower frequencies. Results shown for the higher harmonics need to be interpreted with caution. Although they theoretically meet the Nyquist criterion, the exact amplitude values are subject to noise as data are based on just a few samples per period. The main purpose of the decomposition on the note harmonics is to demonstrate that reed vibration at these harmonics is far smaller than on the fundamental.

B. Single point analysis of vibration cycles

1. Center motion as a function of time

The periodic motion of the reed was found to be highly non-sinusoidal. The shape of the vibration curve depends on which note is excited, blowing pressure, lip force and on mouthpiece design. The acoustic pressure in the instrument and mouthpiece has an important effect on the vibration behavior of the reed, which makes testing of reed vibration under imitation of realistic circumstances and using airflow exited vibration relevant.

Figure 4 showed the position of the back side of the reed tip relative to the mouthpiece, measured on a point at the center and for the reed vibrating at note A4. The reed is practically in contact with the mouthpiece for nearly a quarter of the vibration period: between relative phases $\frac{3\pi}{10}$ and $\frac{\pi}{2}$. Within this contact period, a very small bouncing effect can be seen, with an opening of less than 30μm between the reed and the mouthpiece tip. A similar effect was observed in the simple two-step regime of the clarinet reed (Picart et al., 2007, 2010), where also a small bounce of about 50μm was observed during the closing phase. The curves shown in Figure 4 are similar to the single two-step regime measured by (Colinot et al., 2020) under natural playing conditions. Figure 6 showed the data obtained at note F3. In this case, the special double two-step regime is observed. A bounce effect of 52 μm was seen for the lowest lip force. Within the time resolution of 20 steps per period, no secondary openings are seen when the reed touches the mouthpiece.

The displacement of clarinet reeds in playing conditions lies between 0.1-0.5mm (Bucur, 2019; Gazengel et al., 2016). The order of magnitude of displacement of the alto saxophone reed was the same, yet higher displacements (values up to 0.9mm) were found for different tested notes.

The frequency spectra of different notes revealed that the oscillation of the reed is dominated by the first two or three harmonics. It is beyond the scope of the present study to investigate the effect of different blowing pressures, but this variable can also influence harmonic content of produced sound and reed vibration.

In Section III.A.3., single point measurements were compared between different mouthpieces. Different lip forces had to be used to obtain oscillation which hinders direct comparison. However, Section III.A.2. showed that lip force influences the vibration amplitude, but the shape of the position curve as function of time is largely force independent. Therefore, relevant comparison between mouthpieces can be made despite of the different lip forces used. Figure 7 showed that the time dependence of reed motion is significantly different for the two mouthpieces.

For the different mouthpieces, it was seen that the vibration cycle of the reed attached to a Concept mouthpiece remains closed for a longer fraction of the vibration period as compared to the Spirit mouthpiece. For the Concept mouthpiece, the reed closes for about 35% of the vibration cycle. For the Spirit mouthpiece the closing time is only 25% of the cycle. The Spirit mouthpiece has a markedly larger tip opening (distance between mouthpiece tip and reed in rest position) and different internal geometry than the Concept mouthpiece. The measurements show that this plays an essential role in the motion of the reed.

C. 3D vibrations

1. Effect of lip and mouthpiece

Section III.C examined the full field reed displacement. By analyzing the individual contributions of each frequency component to the total displacement, it is seen that the fundamental frequency component is by far the highest in magnitude. Different musical notes showed different contributions of harmonic content. Figure 9 showed that the shape of the magnitude maps measured for different lip forces on the same mouthpiece are all rather similar, except for the sixth harmonic. Although the Nyquist criterion is still met for this harmonic, the number of time data points becomes low, and additionally the measured amplitude is on the edge of the measuring resolution. Therefore, the result needs to be interpreted with care. Nevertheless, the figure shows that under certain lip forces a higher torsional mode can become apparent in the higher note harmonics, and that such mode is strongly influenced by lip force, but its amplitude is at least a factor of 40 below the amplitude of the simple flexural mode.

(Wilson and Beavers, 1974) found that there are two types of excitable modes at operation in single reed woodwind instruments. The first type is near the natural frequency of the reed and the second type near resonance frequencies of the tube of the instrument which are lower than the reed's natural frequencies. Further they showed that if the reed is lightly damped, the reed will vibrate at its own natural frequencies. The importance of the lip is further explicitly cited. When reeds are heavily damped, instruments such as the saxophone and clarinet operate at resonance frequencies of the instrument's tube. Generally, the air column within the instrument has several natural frequencies, part of them being able to support the auto-oscillation (Facchinetti et al., 2003; Wilson and Beavers, 1974).

(Facchinetti et al., 2003) performed a numerical analysis of the reed and pipe of a clarinet. The modal acoustic pressure at an eigenfrequency of 4119Hz was shown for a reed/mouthpiece system coupled to a short open portion of a pipe. At this mode, a behavior of the reed similar to the first torsional mode was seen. Nonlinear phenomena such as the contact forces between the reed and mouthpiece, as well as lip forces were excluded from the analysis.

In the experimental investigation under mimicked realistic playing conditions, the results indicated that the reed is essentially moving in the simple first bending mode. The first torsional mode was observed in Figure 9 with the lowest lip force. When the lip force was increased, the first torsional mode did not appear in the measurements. The maximum magnitude for the first torsional mode was 0.048 mm measured on the side being 9 times smaller compared to the maximum magnitude at the fundamental f_0.

The magnitude maps at the harmonics which have a major contribution to the motion of the reed, all show a simple in-phase motion over the entire measured surface, corresponding to the first flexural mode. Therefore, the results demonstrate that the behavior of the reed is mainly determined by the first flexural mode of the reed and only marginally by its higher modes. However, by decomposing the full motion of the reed in different harmonic components it was noticed that the reed motion can also to a small extent be influenced by the reed's own resonances.

Many players have the tendency to use softer reeds on mouthpieces with larger openings, but some players also use the same reed strength, or use different strengths on the same mouthpiece depending on playing circumstances and music style. Within the scope of the present paper, it was the aim to demonstrate that mouthpiece geometry can have an important effect on reed vibration.

To focus purely on mouthpiece effect, the data given in Figure 10 were gathered using the same reed strength. For the two mouthpieces, different vibration amplitudes are found, but in both cases the first flexural mode is dominant at all notes. The figure should not be used to draw conclusions concerning mouthpiece performance.

As pointed out in literature (Chaigne and Kergomard, 2016; Fletcher and Rossing, 1998), a mouthpiece with a larger tip opening such as the Spirit mouthpiece needs higher lip pressure or higher blowing pressure, or a combination of both, to initiate auto-oscillation. When using the same reed strength on both mouthpieces, auto-oscillation starts when blowing pressure reduces the reed channel to about one third of the height (relative to the rest state with lip pressure applied). The size of the tip opening therefore is one of the main design parameters of the mouthpiece, together with the distance between the baffle and the backside of the reed. On the Spirit mouthpiece, the vibration amplitude is smaller than on the Concept mouthpiece, but the channel between the reed and the mouthpiece is open for a longer period of time, so these two parameters are strongly inversely correlated. The size of the tip opening is of major importance, and therefore also on the overall vibration behavior of the reed.

In general, the figures demonstrate the important influence of the mouthpiece: both the maximum magnitudes and the spatial distribution of the magnitude over the reed surface differ between the mouthpieces although the reed is driven at the same fundamental frequencies. The relative values of the magnitude at the higher harmonics are also different for both mouthpieces, emphasizing that mouthpiece geometry influences the vibrational behavior of the reed.

2. Magnitude maps at different musical notes

Note frequency sometimes deviates slightly from the defined frequency due to small changes in tuning of the instrument, but the deviation is smaller than 15 cents or about 1% of the note frequency for the Concept mouthpiece for the same lip force. It was shown that the pitch of the instruments can be influenced by the lip force applied as well. The precision of perceptibility in pitch varies largely between human beings. (Loeffler, 2006) explains that humans can distinguish a difference in pitch of about 5–6 cents. The threshold of what is perceptible, known as the just noticeable difference (JND), also varies as a function of the amplitude, the timbre and frequency (Emiroglu, 2007). The precision differs for each individual and depends on the level of training of the auditory skills. In a melodic context, intervals of less than a few cents are imperceptible to the human ear. However, in harmony very small changes can cause large changes in beats and roughness of chords (Benson, 2006).

On the alto saxophone (unlike the clarinet), the fingering (opened and closed tone holes) for notes F3 till Eb4 is the same as for notes F4 till Eb5, apart from one small valve (the "octave valve") in the neck of the instrument which is opened to play the notes F4 till Eb5. A somewhat experienced player can even excite the octave notes without opening the valves (like on the traverse flute), just by changing lip force, air pressure and vocal tract manipulations (Chen et al., 2011; Scavone et al., 2008). The note F5 is again played with the octave valve closed but using an entirely different fingering (side valves on the top part of the saxophone body).

Figure 11 showed that for both mouthpieces the vibration patterns can be divided into two main categories. For F3, the magnitude at the first harmonic can be as large as the fundamental note frequency. For notes F3, A3 and C4 the vibration at the second harmonic is important, with values up to about half of the values at the fundamental. As of F4, when the octave valve is opened, the pattern completely changes and the amplitude at the first harmonic becomes nearly 5 times smaller as compared to the amplitude at the fundamental. For the note F5, which is again played with octave valve but with other fingering than F4, the amplitude at the second harmonic again becomes more important. When exciting the reed at different notes the acoustic feedback of the instrument is altered. The result demonstrates the important influence of the presence of the entire instrument on measured reed vibration.

3. Natural modes

At some of the higher harmonics, more complex distributions of the vibration magnitude are seen, corresponding to higher vibration modes of the reed. In the work of (Taillard et al., 2014), vibrational modes of the clarinet reed were measured and calculated over a broad range of frequencies. Using holographic techniques, (Taillard et al., 2014) measured different vibration modes and their mixtures and showed computational simulations of the different resonance frequencies of the clarinet reed without damping. As an example, four of these simulated results for the clarinet have been added to the supplementary material.[5] The black line in the figure delineates the zone in which measurements were made in the current paper (on saxophone reeds). When comparing this oval-shaped part to the magnitude maps presented in Figure 11, it is seen that the first flexural mode is recognized at all fundamentals and at many harmonics. Further, the measurements show that the first flexural mode is dominant for all notes up till the second harmonic. So, although for F5 the second harmonic is above 2000Hz, the reed is still mainly vibrating in first flexural mode. This possibly happens because of the presence of the lip, making the vibrating part of the reed significantly shorter than for a free vibrating reed and thus pushing the resonance frequencies of higher vibration modes to higher values. The magnitude patterns at the reed tip observed by

(Taillard et al., 2014) for higher vibration modes can be recognized for some of the note harmonics in Figure 11. At the sixth harmonic of A4 (3094Hz) on the Concept mouthpiece, for instance, the typical pattern of the second torsional mode is clearly seen. At some other harmonics, mixtures of higher vibration modes appear. For most of the notes and harmonics, the simple flexure mode is seen, often with a small asymmetry. The distribution of the higher modes over the notes and harmonics is very different for the Spirit and the Concept mouthpiece.

For the Concept mouthpiece the higher harmonics showed a pattern similar to the first torsional mode of the reed. This pattern was also found in the investigations of (Pinard et al., 2003) for free vibrating clarinet reeds. The authors performed a study on the reed's resonances of different reeds and concluded that 'good' and 'very good' reeds show a resonance at the first torsional mode. 'Poor' and 'very poor' reeds did not show a strong resonance at the first torsional mode. The current results show that also in realistic playing conditions the reed motion can be influenced by the natural modes of the reed. This was noticed for example when the reed was mounted on the Concept mouthpiece. When the same reed is mounted on the Spirit mouthpiece, the first torsional mode is no longer excited. On a qualitative level, the reed motion in realistic playing conditions is slightly influenced by the first two transverse modes and generic modes, as seen in the magnitude maps of the higher harmonics.

4. 3D displacement maps as a function of time and lip force

As an example, Mm.1 showed a 3D animated representation of the movement of the reed vibrating on a Spirit mouthpiece at F5. Even at the highest tested note, the reed is still vibrating mainly in its first flexural mode. Figure 11 showed that the higher vibrational modes can be present at some harmonics, but in far smaller amplitude than the first flexural mode. Mm.2 demonstrates that the motion at some of the harmonics becomes much more complicated, but with a very small amplitude. Without decomposition of the vibration onto the harmonics of the played note, the presence of other harmonics is practically impossible to discern in the measured vibration pattern.

Increasing lip force (2.9N-6.7N) slightly increased the playing frequency with 2Hz. In (Benade, 1990), the author stated that changes of the reed's natural frequency (e.g. lip force) can produce small but parallel changes in the air column modes of the instrument that are situated below the reed's natural frequency. The paper explains that these changes become larger for the higher modes that are situated nearer to the reed's natural frequency. The current results demonstrate that increasing lip force has a larger influence on the higher harmonics of the reed motion which lie closer at the eigenfrequencies of the reed.

5. Operational modal analysis

Figures 12 and 13 showed that the first bending mode of the reed is by far the most important, followed by the first torsional mode which has an amplitude of nearly 40 times smaller. On the Concept mouthpiece, the second mode shows a very symmetrical and similar behavior for nearly all tested notes. Only at F5 (see supplementary material) the mode shape differs a bit from simple symmetrical torsion. On the Spirit mouthpiece the second mode shows asymmetric bending at all notes. For some notes the amplitude is largest at the left side of the reed, for others on the right side. In general, on the Spirit mouthpiece all higher modes show more variability between the notes. On both mouthpieces, the vibration modes beyond the first two modes have more complicated patterns. It needs to be noted however that their amplitude is very small and that the calculation is based on the 20 time steps within one vibration period, which increases the uncertainty of the result.

In Figure 13, results obtained for the notes in the lower register of the instrument (F3, A3, C4) are indicated with full lines, the higher notes are indicated with dashed lines. As of the third mode, the relative contribution of the higher operational modes for notes in the higher register decreases less as a function of mode number than for notes in the lower registers. In the Spirit mouthpiece the difference is somewhat less systematic. Between the first and the second mode, the decrease in relative contribution averaged over all notes is a factor of 35.8 ± 9.6 for the Concept mouthpiece and 38.7 ± 13.1 for the Spirit mouthpiece, or 30.8 ± 2.4 dB and 31.3 ± 3.0 dB. As of the second mode, the decrease in relative contribution is nearly linear on the logarithmic scale. For the notes in the lower register the averaged decrease is 6.4dB per mode number and 6.1dB per mode number for the Concept and the Spirit mouthpiece respectively. For the higher register notes this decrease is 4.6dB per mode number and 4.8dB per mode number.

D. Reed vibration profiles along the Y-axis

For the sake of clarity, the Z-axis in Figure 14 was expanded over a factor of 5 with respect to the Y-axis. Consequently, the mouthpiece top profile also looks much more curved than in reality, and openings between the reed and the mouthpiece are exaggerated. Figure 14(a) & (b) show that along its entire visible length (the part that is not covered by the lip), the reed backplane side profile nearly follows the top profile of the mouthpiece when the reed is in its lowest position. Because of the curved shape of the reed tip, the profile measurements at the side start at about 2.5 mm from the origin. At its tip, the reed completely rests on the mouthpiece, but along the Y-direction a small vertical opening between reed and mouthpiece side rails gradually develops. At 7mm from the mouthpiece tip, the opening is about 50 µm wide. Measurements at positions further along the Y-axis were not possible, because there the lip covers the reed front surface.

Figure 14(c) and (d) showed that also at its center profile, the back surface of the reed touches the mouthpiece tip when it is in its lowest position. Further on, the reed backplane is for different time steps even below the surface of the mouthpiece rails, indicating reed bending along the X-axis. Cross sections along the X-axis confirmed the presence of this bending and at position y = 9mm the center of the reed is 70 µm below the top surface defined by the facings of the mouthpiece. This demonstrates that at the lowest position, the motion of the reed becomes distinctly different from what is measured on free vibrating reeds. During this part of the vibration cycle, the boundary conditions change. Before the reed touches the mouthpiece, it has a free boundary condition apart from the zone where it is touched by the lip. In the part of the vibration cycle where the reed is in its lowest position, boundary conditions change from free into supported over a major part of the reed tip circumference. This can be one of the causes why the reed bends along the x-axis.

As a whole, Figure 14 shows that in normal playing conditions, the reed nearly closes against the mouthpiece over its entire circumference but, away from the tip, a thin slit exists between reed and mouthpiece. Through such a slit, air can pass from the mouth to the mouthpiece, which may act as a source noise in the sound of the instrument.

V. CONCLUSION

Full field vibration measurements were shown on the visible part of alto saxophone reeds vibrating under imitation of natural conditions of airflow and lip force. The motion of the reed is highly non-sinusoidal, and the gap between the reed and the mouthpiece can close for a significant part of the vibration cycle. The shape of the mouthpiece and the lip force change both the amplitude of the reed vibration and its harmonic content. For all notes and both mouthpiece shapes, the simple first flexural vibration mode of the reed is predominant, but at higher note harmonics other vibration modes can be present. These modes contribute to the overall timbre of the produced sound. The vibrations of the reed set into motion by airflow and loaded with a visco-elastic lip differ strongly from motions of an acoustically driven free vibrating reed. The acoustic feedback of the instrument, together with the acoustic and hydrodynamic properties of the mouthpiece have an important role on reed vibration. The measurement method allows to study the effect of different mouthpiece geometries and can deliver important data for parametric design improvement of mouthpieces. Previous work has shown that the main difference between high quality artificial reeds and natural cane reeds is the fact that in natural cane the Youngs modulus in transversal direction is much smaller than in longitudinal direction. As the current work shows that the first bending mode is far more important than any of the higher reed modes, this could indicate that the ratio of longitudinal versus transversal stiffness is not of major importance. This can be a reason why artificial reeds perform well, despite of the important difference in transversal stiffness with natural reeds.

Coming back to the research questions, the conclusions can by summarized as follows:

- Under airflow-induced auto oscillation and in presence of lip force, mouthpiece and instrument, the reed vibrates mainly in its simple first flexural mode for all note pitches. This is very different form the vibrations observed on free vibrating reeds. Amplitudes of higher vibration modes observed at note harmonics are at least a factor of 8 smaller than the amplitude of the first flexural mode. The operational modal analysis showed that higher modes have a nearly 40 times smaller contribution compared to the first operational mode which is the first flexural mode of the reed.

- The primary influence of mouthpiece geometry and lip force is on the amplitude of the reed motion, but effects are also present on the 3D amplitude maps at the higher harmonics of the played note.
- During a major part of the vibration cycle, the reed tip closes against the mouthpiece. For positions away from the tip, a small gap develops between reed and mouthpiece upper surface.
- As the reed mainly vibrates in its first flexural mode for all notes, a single point measurement can be used as a good first-order representation of reed motion at all note pitches.

ACKNOWLEDGEMENTS

We gratefully acknowledge the support of J. Cottier and B. Andrieux (Henri Selmer, Paris, France) for putting the test mouthpieces to our disposal, and S. King and M. Kortschot (Légère Reed Ltd., Barrie, Ontario, Canada) for putting reeds to our disposal.

SUPPLEMENTAL FILES

[1] See supplementary material at [URL will be inserted by AIP] for the measurement precision of the DIC algorithm for an out of plane displacement caused by a uniform translation of 700 μm. SuppPub.1

[2] See supplementary material at [URL will be inserted by AIP] for full field animations of reed motion for different musical notes. SuppPubmm1-13.

[3] See supplementary material at [URL will be inserted by AIP] for magnitude maps of reed vibration at the fundamental and the first 6 harmonic components, with the reed mounted on the Spirit mouthpiece, with applied lip force of 9.6N. SuppPub.2

[4] See supplementary material at [URL will be inserted by AIP] for mode shapes of the first seven operational modes of the reed vibrating on the Concept and Spirit for different notes. The color scales only display the shape of the mode. The first operational mode is the simple bending mode. The second mode is a torsional mode for most of the tested notes. Higher modes are more complicated. SuppPub. 3 & 4

[5] See supplementary material at [URL will be inserted by AIP] for simulated natural modes of a clarinet reed (results from the paper by (Taillard et al., 2014) reprinted with permission of the authors.). The black line delineates the portion of the reed on which measurements were made in the current paper. (a) first flexural mode, (b) first torsional mode, (c) second torsional mode, (d) second generic mode magnitude distributions. SuppPub. 5

REFERENCES

Almeida, A., George, D., Smith, J., and Wolfe, J. (**2013**). "The clarinet: How blowing pressure, lip force, lip position and reed 'hardness' affect pitch, sound level, and spectrum," J. Acoust. Soc. Am., **134**, 2247–2255. doi:10.1121/1.4816538

Backus, J. (**1961**). "Vibrations of the Reed and the Air Column in the Clarinet," J. Acoust. Soc. Am.,.

Balcaen, R., Reu, P. L., Lava, P., and Debruyne, D. (**2017**). "Stereo-DIC Uncertainty Quantification based on Simulated Images," Exp. Mech., **57**, 939–951. doi:10.1007/s11340-017-0288-9

Benade, A. H. (**1990**). *Fundamentals of musical acoustics*, Dover Publications Inc., Second Edi., 596 pages.

Benade, A. H., and Gans, D. J. (**1968**). "Sound Production in Wind Instruments," Ann. N. Y. Acad. Sci., **155**, 247–263. doi:10.1111/j.1749-6632.1968.tb56770.x

Benson, D. (**2006**). *Music: A Mathematical Offering*, Cambridge University Press, Cambridge. doi:10.1017/CBO9780511811722

Bornert, M., Hild, F., Orteu, J.-J., and Roux, S. (**2012**). "Digital Image Correlation," In M. Grédiac, F. Hild, and A. Pineau (Eds.), Full-Field Meas. Identif. Solid Mech., John Wiley & Sons, Inc., Hoboken, NJ USA, pp. 157–190. doi:10.1002/9781118578469.ch6

Brincker, R. (**2015**). *Introduction to Operational Modal Analysis*, John Wiley & Sons, Inc.

Bucur, V. (**2019**). *Handbook of materials for wind musical instruments*, Handb. Mater. Wind Music. Instrum., Springer Nature Switzerland, 1–819 pages. doi:10.1007/978-3-030-19175-7

Campbell, D. M. (**1999**). "Nonlinear dynamics of musical reed and brass wind instruments," Contemp. Phys.,. doi:10.1080/001075199181305

Chaigne, A., and Kergomard, J. (**2016**). *Acoustics of Musical Instruments*, Modern Acoustics and Signal Processing, Springer New York, New York, NY. doi:10.1007/978-1-4939-3679-3

Chen, J. ming (**2009**). *Vocal Tract Interactions in Woodwind Performance* (PhD thesis), University of New South Wales.

Chen, J.-M., Smith, J., and Wolfe, J. (**2011**). "Saxophonists tune vocal tract resonances in advanced performance techniques," J. Acoust. Soc. Am., **129**, 415–426. doi:10.1121/1.3514423

Colinot, T., Guillemain, P., Vergez, C., Doc, J.-B., and Sanchez, P. (**2020**). "Multiple two-step oscillation regimes produced by the alto saxophone," J. Acoust. Soc. Am., **147**, 2406–2413. doi:10.1121/10.0001109

Emiroglu, S. S. (**2007**). *Timbre perception and object separation with normal and impaired hearing* (PhD thesis), Carl-von-Ossietzky-Universität, Oldenburg.

Fabre, B., Gilbert, J., Hirschberg, A., and Pelorson, X. (**2011**). "Aeroacoustics of musical instruments," Annu. Rev. Fluid Mech., **44**, 1–25. doi:10.1146/annurev-fluid-120710-101031

Facchinetti, M. L., Boutillon, X., and Constantinescu, A. (**2003**). "Numerical and experimental modal analysis of the reed and pipe of a clarinet," J. Acoust. Soc. Am., **113**, 2874–2883. doi:10.1121/1.1560212

Fadhil Shazmir, M., Ayuni Safari, N., Azhan Anuar, M., A.Mat Isa, A., and A.R, Z. (**2018**). "Operational Modal Analysis on a 3D Scaled Model of a 3-Storey Aluminium Structure," Int. J. Eng. Technol., **7**, 78. doi:10.14419/ijet.v7i4.27.22485

Fletcher, N. H. (**1978**). "Mode locking in nonlinearly excited inharmonic musical oscillators," J. Acoust. Soc. Am.,.

Fletcher, N. H., and Rossing, T. D. (**1998**). *The Physics of Musical Instruments*, Springer New York, New York, NY. doi:10.1007/978-0-387-21603-4

Fuks, L., and Sundberg, J. (**1999**). "Blowing pressures in bassoon, clarinet, oboe and saxophone," Acustica, **85**, 267–277.

Gazengel, B., Dalmont, J. P., and Petiot, J. F. (**2016**). "Link between objective and subjective characterizations of Bb clarinet reeds," Appl. Acoust., **106**, 155–166. doi:10.1016/j.apacoust.2015.12.015

Kobata, T., and Idogawa, T. (**1993**). "Pressure in the mouthpiece, reed opening, and air-flow speed at the reed opening of a clarinet artificially blown," J. Acoust. Soc. Jpn. E, **14**, 417–428. doi:10.1250/ast.14.417

Loeffler, D. B. (**2006**). *Instrument Timbres and Pitch Estimation in Polyphonic Music* (Thesis), Georgia Institute of Technology. Retrieved from https://smartech.gatech.edu/handle/1853/10568

Mayer, A. (**2003**). "Riam (Reed instrument artificial mouth) A computer controlled excitation device for reed instruments," Proc. Stockh. Music Acoust. Conf.,.

Nederveen, C. J. (**1969**). *Acoustical Aspects of Woodwind Instruments*.

Pan, B., Lu, Z., and Xie, H. (**2010**). "Mean intensity gradient: An effective global parameter for quality assessment of the speckle patterns used in digital image correlation," Opt. Lasers Eng., **48**, 469–477. doi:10.1016/j.optlaseng.2009.08.010

Pan, B., Qian, K., Xie, H., and Asundi, A. (**2009**). "Two-dimensional digital image correlation for in-plane displacement and strain measurement: a review," Meas. Sci. Technol., **20**, 062001. doi:10.1088/0957-0233/20/6/062001

Picart, P., Leval, J., Piquet, F., Boileau, J. P., Guimezanes, T., and Dalmont, J. P. (**2010**). "Study of the mechanical behaviour of a clarinet reed under forced and auto-oscillations with digital fresnel holography," Strain, **46**, 89–100. doi:10.1111/j.1475-1305.2008.00593.x

Picart, P., Leval, J., Piquet, F., Boileau, J. P., Guimezanes, T., and Dalmont, J.-P. (**2007**). "Tracking high amplitude auto-oscillations with digital Fresnel holograms," Opt. Express, **15**, 8263. doi:10.1364/oe.15.008263

Pinard, F., Laine, B., and Vach, H. (**2003**). "Musical quality assessment of clarinet reeds using optical holography," J. Acoust. Soc. Am., **113**, 1736–1742. doi:10.1121/1.1543586

Reu, P. (**2013**). "Stereo-rig design: Stereo-angle selection - Part 4," Exp. Tech., **37**, 1–2. doi:10.1111/ext.12006

Reu, P. L., Sweatt, W., Miller, T., and Fleming, D. (**2015**). "Camera System Resolution and its Influence on Digital Image Correlation," Exp. Mech., **55**, 9–25. doi:10.1007/s11340-014-9886-y

Scavone, G. P., Lefebvre, A., and da Silva, A. R. (**2008**). "Measurement of vocal-tract influence during saxophone performance," J. Acoust. Soc. Am., **123**, 2391–2400. doi:10.1121/1.2839900

Sutton, M. A., Orteu, J. J., and Schreier, H. (**2009**). *Image Correlation for Shape, Motion and Deformation Measurements: Basic Concepts,Theory and Applications*, Springer US. doi:10.1007/978-0-387-78747-3

Taillard, P. A., Laloë, F., Gross, M., Dalmont, J. P., and Kergomard, J. (**2014**). "Statistical estimation of mechanical parameters of clarinet reeds using experimental and numerical approaches," Acta Acust. United Acust., **100**, 555–573. doi:10.3813/AAA.918735

Ukshini, E., and Dirckx, J. J. J. (**2020**). "Longitudinal and transversal elasticity of natural and artificial materials for musical instrument reeds," Materials, **13**, 1–13. doi:10.3390/ma13204566

Ukshini, E., and Dirckx, J. J. J. (**2021**). "Setup for musical reed instrument testing using constant phase stroboscopic imaging," Opt. Eng., , doi: 10.1117/1.OE.60.4.044105. doi:10.1117/1.OE.60.4.044105

Wang, S., Maestre, E., and Scavone, G. (**2021**). "Acoustical modeling of the saxophone mouthpiece as a transfer matrix," J. Acoust. Soc. Am., **149**, 1901–1912. doi:10.1121/10.0003814

Wilson, T. A., and Beavers, G. S. (**1974**). "Operating modes of the clarinet," J. Acoust. Soc. Am., **56**, 653–658. doi:10.1121/1.1903304

FIGURE CAPTIONS

Figure 1: Top view schematic representation of the measurement setup. Two cameras (C1 & C2) observe the reed motion. The mouthpiece is positioned inside a pressurized transparent box and is turned in such a way that the reed faces the cameras. (color online)

Figure 2: Coordinate system in which the data is presented in. The origin of the x-axis is set at the middle of the mouthpiece tip. The z- axis is chosen perpendicular to the surface of the mouthpiece table, with its origin at the level of the mouthpiece tip. The dotted line indicates the level of the mouthpiece table. (color online)

Figure 3: Top view on a reed with the artificial lip in place. The black line indicates the circumference of the zone in which 3D vibration data are measured. The dotted lines indicate the locations of cross sections along which reed motion will be shown (Section III.C). The artificial lip is indicated with gray. (color online)

Figure 4: Position of the backside of the reed tip center as a function of time measured at note A4 for three different lip forces on a reed mounted on the Concept mouthpiece. Measurements are repeated using three different reeds with the same nominal strength. Repeat measurements are indicated using the same markers and line colors. (color online)

Figure 5: Frequency spectra for A4 measured at (a) the vicinity of the reed tip and (b) bottom left side of the reed. The fundamental and the first six harmonics are shown. Different markers are used

to show the different lip forces. Repeat measurements with different reeds are indicated by the same markers. The DC component is shown as well. (color online)

Figure 6: Position of the backside of the reed tip center as a function of time measured at note F3 for two different lip forces on a reed mounted on the Concept mouthpiece. The markers indicate the measured time steps. The double two-step vibration regime is seen. (color online)

Figure 7: Position of the reed bottom for different lip forces and different mouthpieces measured at note A4. When the reed is attached to the Concept mouthpiece the reed gap remains closed for a longer fraction of the vibration period than when the reed is mounted on the Spirit mouthpiece. (color online)

Figure 8: Position of the backside of the reed tip center as a function of vibration phase measured at note C5. Dots and triangles indicate the time steps at which measurements were made (subsequent gray values and symbols correspond to reed cross sections shown in Figure 14) and are labeled from 0 to 20. Each subsequent time step number corresponds to a phase increase of $2\pi/20$. The reed tip nearly touches the mouthpiece for more than a quarter of the vibration period. (color online)

Figure 9: Measured magnitude maps (first row) and their decomposition on the fundamental and first six harmonic components for the reed vibrating at A4 on a Concept mouthpiece with different lip forces applied. The simple up-and-down movement of the first fundamental is by far the most important component in the motion, but higher vibration modes are also present and differ in relative amplitude depending on lip force. The most right column shows a repeat measurement on a different reed using approximately the same reed force as used for the data shown in the second column. (color online)

Figure 10: Measured magnitude maps (first row) and their decomposition on the fundamental and first six harmonic components for the reed vibrating at C5 on a Concept and Spirit mouthpiece. On the Spirit mouthpiece a higher lip force is needed and vibration magnitude is smaller than on the Concept mouthpiece. The contribution at f_4 is however much higher on the Spirit mouthpiece. (color online)

Figure 11: Measured magnitude maps (first row) and their decomposition on the fundamental and first six harmonic components, with the reed mounted on the Concept mouthpiece, with lip force applied of 2.9N. (color online)

Figure 12: Shape of the first seven operational modes of the reed vibrating on the Concept (left column) and Spirit (right column) mouthpiece, for note C5. The grayscales (color online) only display the shape of the mode. On both mouthpieces, the first operational mode is the simple bending mode. The second mode is a torsional mode. Higher modes are more complicated. (color online)

Figure 13: Relative contribution of the first seven operational modes for (a) Concept mouthpiece, (b) Spirit mouthpiece shown in Fig. 12. Results for notes in the lower register of the instrument are indicated by full lines, results for notes in the higher register are indicated by dashed lines. Because values decrease dramatically with mode number, results are shown on a logarithmic scale. The amplitude of the second mode is nearly 40 times smaller than the amplitude of the first mode. Values haven been normalized with respect to the value at the first mode. (color online)

Figure 14: cross sections along the Y-axis of the back side of the reed, measured at the subsequent time steps indicated in Figure 8. Top row shows motion of the section taken at the side of the reed, bottom row shows motion of the section at the center of the reed (location of the section as indicated in Fig. 3). Left and right panel respectively show the first and second half of the vibration cycle. To better distinguish subsequent curves, data obtained at even time points are indicated with dashed lines and data at odd time points are indicated using full lines. The black zone indicates the mouthpiece material at the location of the section. The gray zone indicates the projection of the mouthpiece shape onto the Y-Z plane. The position of the start of the lip is indicated by arrows. (color online)